ACS Energy LETTERS

http://pubs.acs.org/journal/aelccp

LETTER

Molecular Tailoring of Phenothiazine-Based Hole-Transporting Materials for High-Performing Perovskite Solar Cells

Roberto Grisorio,*[,†,‡] Bart Roose,[§] Silvia Colella,[‡,∥] Andrea Listorti,[‡,∥] Gian Paolo Suranna,[†,‡] and Antonio Abate*[,§,⊥]

[†]Dipartimento di Ingegneria Civile, Ambientale, del Territorio, Edile e di Chimica (DICATECh), Politecnico di Bari, Via Orabona 4, 70125 Bari, Italy

[‡]CNR NANOTEC − Istituto di Nanotecnologia, Via Monteroni, 73100 Lecce, Italy

[§]Adolphe Merkle Institute, Chemin des Verdiers 4, CH-1700 Fribourg, Switzerland

[∥]Dipartimento di Matematica e Fisica "E. De Giorgi", Università del Salento, Via per Arnesano, 73100 Lecce, Italy

[⊥]Young Investigator Group Active Materials and Interfaces for Stable Perovskite Solar Cells, Helmholtz-Zentrum Berlin für Materialien und Energie, Kekuléstrasse 5, 12489 Berlin, Germany

Supporting Information

ABSTRACT: **Phenothiazine-based compounds, PTZ1 and PTZ2, were synthesized through straightforward Buchwald−Hartwig and Suzuki−Miyaura cross-couplings, respectively, by binding the suitable donor groups (diarylamine or triarylamine) to a phenothiazine core. Phenothiazine-based structures were proven for the first time as hole-transporting materials in solution-processed lead trihalide perovskite-based solar cells. A dramatic effect exerted by the presence of phenylene spacers was observed on the relevant photovoltaic performances. The power conversion efficiencies measured under AM1.5 sun increase from 2.1% (PTZ1) to a remarkable 17.6% (PTZ2), a value rivaling those obtained with the state-of-the-art Spiro-OMeTAD (17.7%). These results indicate phenothiazine-based compounds as promising candidates to be used as readily available and cost-effective hole-transporting materials in perovskite solar cells.**

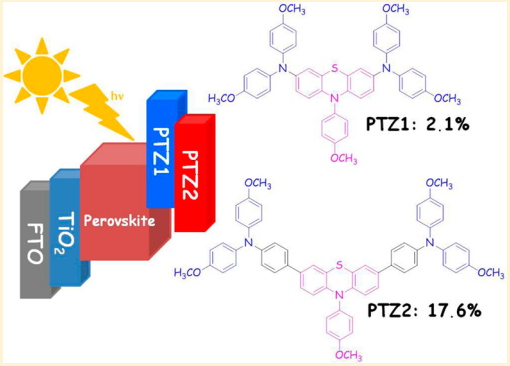

Since the pioneering report by Miyasaka et al. in 2009,[1] organic−inorganic perovskites have rapidly become the hottest topic in photovoltaics because of their excellent intrinsic properties, such as light-harvesting from visible to near-infrared wavelengths with high extinction coefficients and long electron−hole diffusion lengths.[2−5] The best-performing device configuration for perovskite-based solar cells (PSCs) comprises a perovskite layer sandwiched between an electron and hole transporting material (HTM).[6] While power conversion efficiencies (PCE) of ∼10% have been reported for PSC deprived of the HTM layer, in the highest-performance PSCs, the free photogenerated holes within the perovskite material need to be extracted and transported by efficient HTMs.

Numerous organic small molecules have been investigated as HTM in PSCs. To date, the highest reported PCE values (over 20%) have been reached with molecules, such as Spiro-OMeTAD and FDT, sharing the spiro functionality as common structural feature.[7] However, the multistep synthesis of the spiro *motif* is prohibitively expensive and challenging, because it requires low temperature and harsh acid and basic conditions. Moreover, high-purity sublimation-grade of commercial Spiro-OMeTAD is commonly required to obtain high-performance devices. For these reasons, alternative building blocks have been used as cores aiming at reaching state-of-the-art photovoltaic figures of merit in PSCs, such as thiophene derivatives,[8] triphenylamine,[9] bridged-triphenylamines,[10] pyrene,[11] 3,4-ethylenedioxythiophene,[12] linear π-conjugated systems,[13] triptycene,[14] silolothiophene,[15] tetraphenylethene,[16] and triazines,[17] all of them suitably decorated with diarylamines, triarylamines, and/or carbazole side groups. Furthermore, there are also examples of HTMs incorporating phenoxazine,[18] pentacene,[19] benzo-dithiophene derivatives,[20] and *S*,*N*-heteropentacene[21] as cores with absorption in the visible and near-infrared region, which have exhibited PCEs higher than 15%.

Received: January 18, 2017
Accepted: April 10, 2017
Published: April 10, 2017

DOI: 10.1021/acsenergylett.7b00054
ACS Energy Lett. 2017, 2, 1029−1034

Scheme 1. Synthetic Sequence for Obtaining PTZ1 and PTZ2[a]

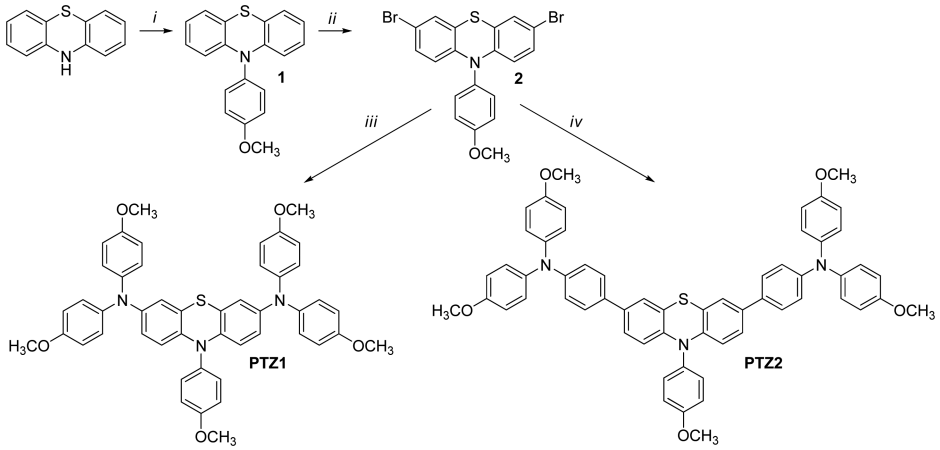

[a](*i*) 4-bromoanisole, $Pd(AcO)_2$/dppf, *tert*-BuONa, toluene, 100 °C; (*ii*) NBS, chloroform; (*iii*) *p*-methoxy-diphenylamine, $Pd(AcO)_2$/dppf, *tert*-BuONa, toluene, 100 °C; (*iv*) 4-methoxy-*N*-(4-methoxyphenyl)-*N*-(4-(4,4,5,5-tetramethyl-1,3,2-dioxaborolan-2-yl)phenyl)aniline, $Pd(PPh_3)_4$, 2M K_2CO_3, toluene, reflux.

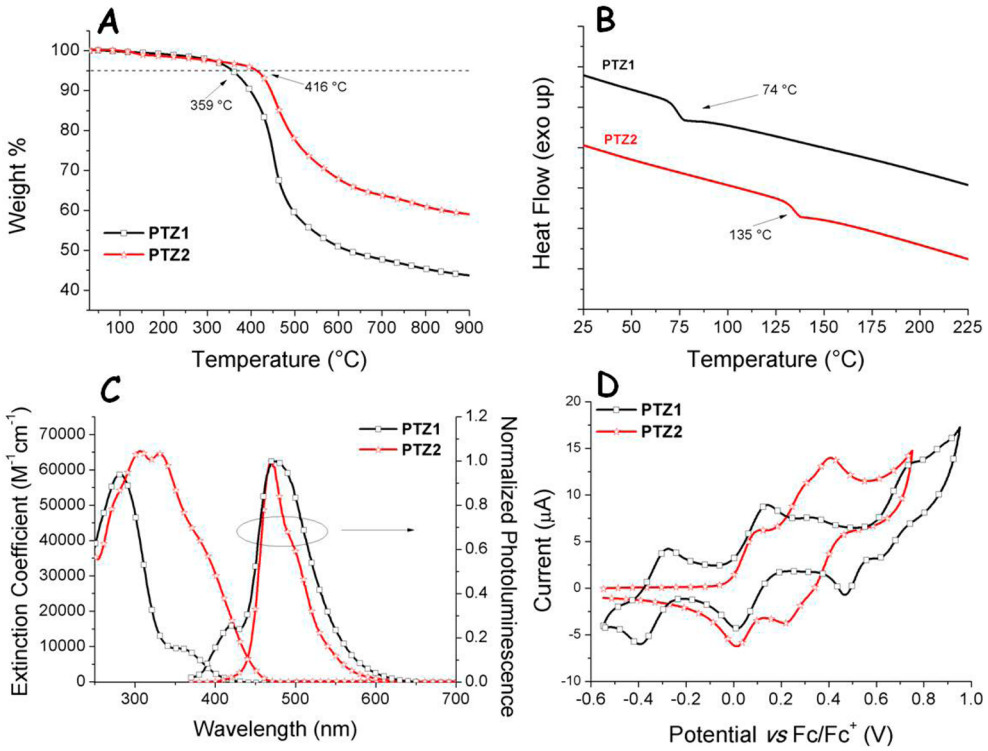

Figure 1. (A) Thermogravimetric analysis of PTZ1 and PTZ2 measured with a heating rate of 10 °C min^{-1}. (B) Second DSC heating traces of HTMs previously heatied and cooled with a scan rate of 10 °C min^{-1} under nitrogen atmosphere. (C) Absorption spectra of PTZ1 and PTZ2 recorded in dichloromethane (3.0×10^{-5} M) and normalized photoluminescence spectra (λ_{ex} = 350 nm). (D) Cyclic voltammograms of HTMs in dichloromethane solutions (1.0×10^{-4} M) using Bu_4NBF_4 (0.1 M) as the supporting electrolyte.

On the basis of the current interest toward carbazole- and fluorene-based cores in designing high-performing HTMs,[22−27] we deemed it worthwhile to investigate the use of the phenothiazine building block as a structural variant for the construction of molecularly engineered HTMs (**PTZ1** and **PTZ2**, Scheme 1). Phenothiazine is a low-cost and flexible electron-rich heteroaromatic unit, which provides access to a wide library of HTMs by relatively cheap synthetic procedures. The fundamental properties of the proposed phenothiazine-based HTMs were found to be strongly dependent on the presence of a π-bridge between the donor groups and the phenothiazine core, which literally boosts the **PTZ2** performance in PSCs *on par* with that of the Spiro-OMeTAD reference, providing solid ground for further investigations and potential improvements.

The phenothiazine-based core was obtained in a two-step synthetic sequence starting from commercial sources (Scheme 1). A palladium-catalyzed cross-coupling reaction between phenothiazine and 4-bromoanisole was used to protect the nitrogen atom of the core affording the intermediate **1**, while the bromo-derivative **2** was obtained by reaction of **1** with *N*-bromo-succinimide. The target molecule **PTZ1** was prepared

DOI: 10.1021/acsenergylett.7b00054
ACS Energy Lett. 2017, 2, 1029−1034

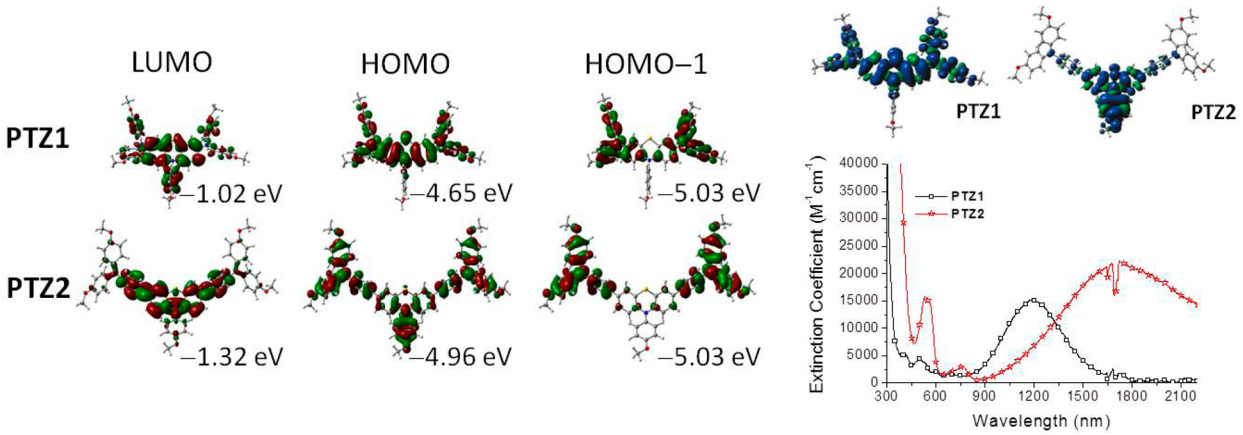

Figure 2. (Left) Isodensity plots of the LUMO, HOMO, and HOMO−1 for PTZ1 and PTZ2 and the corresponding DFT-calculated energies of HOMO and HOMO−1 at the B3LYP/6-311G(d,p) level of theory including solvent effects (CH_2Cl_2) using nonequilibrium implementation of the conductor-like polarizable continuum model. (Right) DFT-calculated electron spin density distributions of PTZ1$^{\bullet+}$ and PTZ2$^{\bullet+}$ (in the doublet state) at the UCAM-B3LYP/6-31G(d,p) level of theory (top) and ultraviolet−visible−near-infrared spectra of PTZ1 and PTZ2 solutions (3.0×10^{-5} M in dichloromethane) upon equimolar addition of the FK209-dopant (bottom).

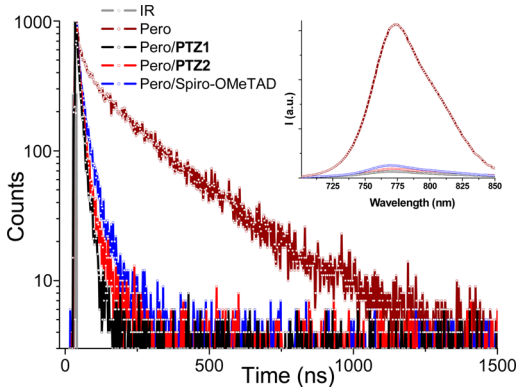

Figure 3. Time-resolved photoluminescence measurements of glass/Pero/PMMA (wine line), glass/Pero/PTZ1 (red line), glass/Pero/PTZ2 (black line), and glass/Pero/Spiro-OMeTAD (blue line). The decays were collected at the maximum of the perovskite emission band (780 nm, excited at 645 nm). Inset: photoluminescence spectra of glass/Pero/PMMA (wine line), glass/Pero/PTZ1 (red line), glass/Pero/PTZ2 (black line), and glass/Pero/Spiro-OMeTAD (blue line).

Table 1. Photovoltaic Parameters[a] Extracted from the *J*−*V* Curves in Figure 4

HTM	V_{OC} (V)	J_{SC} (mA/cm^2)	FF	PCE (%)
PTZ1	0.82	4.2	0.61	2.1
PTZ2	1.11	21.1	0.75	17.6
Spiro-OMeTAD	1.15	21.6	0.71	17.7

[a]Open-circuit voltage (V_{OC}), short circuit current (J_{SC}), fill factor (FF), and power conversion efficiency (PCE).

via a Buchwald−Hartwig C−N cross coupling between **2** and *p*-methoxy-diphenylamine in the presence of $Pd(AcO)_2$/dppf as the catalytic system, *tert*-BuONa as the base, and toluene as the solvent in 71% yield. The variant **PTZ2** was synthesized via a Suzuki−Miyaura C−C cross coupling between **2** and 4-methoxy-*N*-(4-methoxyphenyl)-*N*-(4-(4,4,5,5-tetramethyl-1,3,2-dioxaborolan-2-yl)phenyl)aniline in the presence of $Pd(PPh_3)_4$ as the catalytic system, a 2 M K_2CO_3 aqueous solution acting as the base, and toluene as the solvent in 81% yield. The introduction of 4-methoxyphenyl group on the phenothiazine core was conceived to impart the necessary thermal stability to the corresponding material and warrant the

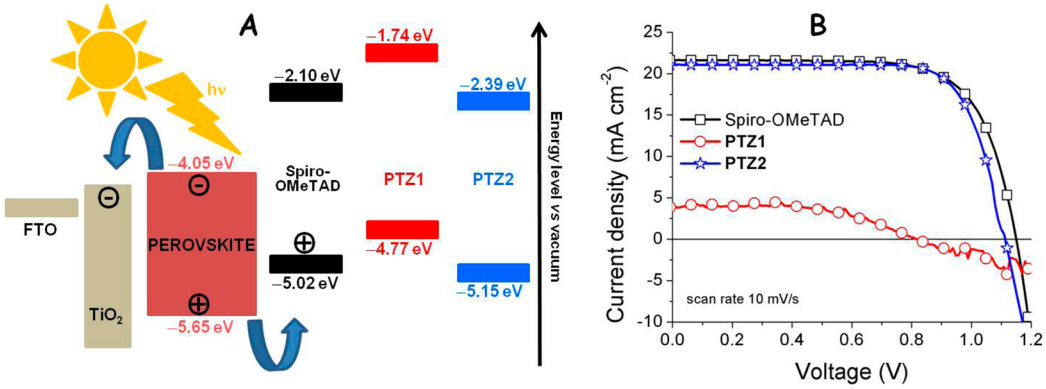

Figure 4. (A) Energy level diagram of the PSC components. (B) Current density−voltage (*J*−*V*) curves for a perovskite solar cell prepared with PTZ1, PTZ2, and Spiro-OMeTAD as HTM. The *J*−*V* curves were measured at a scan rate of 10 mV/s from forward bias to short-circuit condition under AM1.5 simulated solar light illumination. The devices were not preconditioned under light or voltage bias before each *J*−*V* scan. The active area was defined by a shadow mask with an aperture of 0.1 cm^2.

DOI: 10.1021/acsenergylett.7b00054
ACS Energy Lett. 2017, 2, 1029−1034

formation of an amorphous thin film (vide infra). The synthetic details, primary characterization, and estimate of the chemical costs[28] for **PTZ1** and **PTZ2** are reported in the Supporting Information. It is worth noting that the synthesis cost of **PTZ1** and **PTZ2** (111.90 $/g and 156.76 $/g respectively) were found to be remarkably lower than that of Spiro-OMeTAD (~600 $/g).[29]

The thermal behavior of **PTZ1** and **PTZ2** was assessed by thermogravimetric analysis (TGA) and differential scanning calorimetry (DSC) measurements. A satisfactory thermal stability was evidenced by TGA: it was found that **PTZ1** exhibits a decomposition temperature at 359 °C, whereas in the case of **PTZ2**, it was observed at 416 °C (Figure 1A). This value is slightly lower than that of Spiro-OMeTAD (424 °C). The thermal transitions of **PTZ1** and **PTZ2** were studied by DSC, and the obtained data were compared with those of Spiro-OMeTAD (Figure 1B).[27] During the first heating scan, glass transitions accompanied by enthalpic relaxation were observed for **PTZ1** and **PTZ2** and no melting processes were recorded, indicating that the materials exist in an amorphous state. No crystallization was observed during the cooling and second heating steps; only the glass transition was observed at 74 and 135 °C for **PTZ1** and **PTZ2**, respectively. On the basis of these results, it can be stated that **PTZ2** is more stable in the amorphous state with respect to that of Spiro-OMeTAD (glass transition temperature: 125 °C), making it particularly relevant for photovoltaic applications.[15,30]

The normalized ultraviolet−visible absorption spectra **PTZ1** and **PTZ2** in CH_2Cl_2 are shown in Figure 1C. It is worth noting that the two absorption profiles are completely different, because **PTZ1** shows an absorption maximum at 282 nm with a shoulder at longer wavelengths, while **PTZ2** exhibits two distinct absorption maxima at 308 and 332 nm. The optical band gaps determined from the onset of absorption are 410 nm for **PTZ1** and 449 nm for **PTZ2** and are consistent with the different conjugation extension of the two molecules. Meanwhile, the emission spectra for **PTZ1** and **PTZ2** show fluorescence peaks at 475 and 470 nm, respectively.

The oxidation potentials of **PTZ1** and **PTZ2** should be suitable with respect to the perovskite energy levels in order to keep a high open-circuit voltage (V_{OC}) of the device and to warrant an efficient interfacial hole transfer kinetics. The HOMO levels of the new HTMs were determined by cyclic voltammograms (CVs), which are shown in Figure 1D. On the basis of the electrochemical data, the highest-occupied molecular orbitals (HOMOs) of the molecules have been estimated as −4.77 eV for **PTZ1** and −5.15 eV for **PTZ2** in solution, whereas, in the same conditions, Spiro-OMeTAD exhibited a value of −5.02 eV. The higher oxidation potential for **PTZ2** could be favorable for obtaining a high V_{OC} in PSCs, while the relatively lower oxidation potential of **PTZ1** could result in a faster hole transfer between the perovskite layer and the HTM.[31] The oxidation potential trend is in good accordance with the results of the density functional theory (DFT) calculations, corroborating the observation that the HOMO of **PTZ2** is substantially stabilized by the introduction of the phenylene spacers. It is worth noting that the lowest unoccupied molecular orbitals (LUMOs) of **PTZ1** and **PTZ2** are mainly localized on the phenothiazine core, whereas the electron density of the relevant HOMOs differs significantly. While the HOMO of **PTZ1** is mainly localized on the phenothiazine core and part of the two diarylamine groups, the HOMO of **PTZ2** is prevalently distributed (Figure 2) on the three arylamine groups of the structure, despite the dihedral distortion introduced by the presence of the phenylene moieties (Figure S5).

Although electrochemical measurements and theoretical calculations provide qualitative information about ground-state electron density distribution of the HTMs under investigation, information about hole delocalization within the molecular structure in its radical cation form (p-type doping) is crucial to represent a plausible scenario concerning hole hopping and, more generally, to draw the structure−property relationships needed for the molecular design of new HTMs. To test the response of **PTZ1** and **PTZ2** to the p-type doping, their absorption spectra were measured in the presence of an equimolar amount of the cobalt(III)-complex (FK209), which is used as a dopant in the device construction. This experiment not only reveals the effective p-doping of potential HTMs by FK209 for increasing the positive charge carrier density but also offers a tool to represent the charge distribution in the relevant radical cations. In the case of **PTZ1**, new absorption at 500 nm appears upon chemical oxidation and, more importantly, a relatively strong band crops up at 1194 nm (Figure 2). With the aid of TD-DFT calculations (Figure S6), this low-energy band was attributed to the amine → phenothiazine$^{\bullet+}$ charge-transfer transition, suggesting the prevalent charge localization of **PTZ1**$^{\bullet+}$ on the phenothiazine core. In spite of its remarkably higher oxidation potential, also in the case of **PTZ2** the observed spectral changes upon chemical oxidation confirm the p-doping of the molecule by FK209, because two relatively intense bands appear at 539 and 1714 nm (Figure 2). The broad lower-energy absorption can be reasonably ascribed to amine → amine$^{\bullet+}$ charge-transfer transition in the case of **PTZ2**$^{\bullet+}$, as suggested by theoretical calculations (Figure S6), while its electron spin density distribution is prevalently localized on the *p*-anisyl-phenothiazine system (Figure 2). On the basis of these results, we can anticipate that the strong charge localization in **PTZ1** (with respect to **PTZ2**) in its radical cation state may result in a rapid oxidative degradation of the molecule during the device operation.

We scrutinized the charge extraction process at the perovskite/HTM interface performing steady-state and time-resolved photoluminescence analyses.[32] When a film of Spiro-OMeTAD, **PTZ1**, or **PTZ2** was deposited on the perovskite layer, its steady-state radiative emission was severely quenched, suggesting that our phenothiazine-based compounds efficiently extract the photogenerated holes from the light-absorbing active layer (inset of Figure 3). The quantification of the hole extraction process was carried out by time-resolved analyses (Figure 3), and the radiative lifetimes retrieved with double-exponential fitting of the curves are reported in Table S1. The photoluminescence quenching activity is stronger in the case of **PTZ1** in line with its lowest oxidation potential.

On the basis of these results, we fabricated state-of-the-art PSCs under inert atmosphere, using a lead-based mixed halide (bromine and iodine) and cation (methylammonium, formamidinium, and cesium) perovskite, as reported in the most recent literature.[33] Figure 4 displays the current density−voltage (J−V) curves of the PSCs prepared with **PTZ1**, **PTZ2**, and Spiro-OMeTAD as HTMs and their energy level diagram in comparison with the other solar cell components. The corresponding device performance parameters are listed in Table 1. It can be observed that **PTZ2** performs similarly to the Spiro-OMeTAD device, with a power conversion efficiency (PCE) above 17.5%. The short-circuit currents (J_{SC}) are quite

DOI: 10.1021/acsenergylett.7b00054
ACS Energy Lett. 2017, 2, 1029−1034

similar, while the open-circuit voltage (V_{OC}) and the fill factor (FF) are slightly higher for Spiro-OMeTAD and **PTZ2**, respectively. The higher FF of the **PTZ2** can be in part attributed to the higher conductivity of the HTM layer (Figure S7). Conversely, the PSC employing **PTZ1** as HTM showed rather poor performances (PCE = 2.1%), which we rationalized as the result of oxidative degradation due to the low oxidation potential of the molecule (see the Supporting Information). It can be noted that $J-V$ curves have been collected with a voltage scan rate of 10 mV/s, which has been proven to be an optimum value to currently estimate the efficiency of PSCs.[34]

In conclusion, we demonstrated that the minor structural difference between **PTZ1** and **PTZ2** dramatically influenced molecular geometry and optoelectronic parameters of relevance for HTMs in perovskite solar cells. We were able to deeply influence ground-state electron density and electron spin density distribution as well as potential ionization of these HTMs by spacing the dianisyl-amine donor groups from the phenothiazine core by phenylene units. The dramatic difference in photovoltaic performances exhibited by the two phenothiazine-based derivatives can be attributed to the modulation of electron density distribution, which controls the stability of molecules during the charge-transfer dynamics at the perovskite/HTM interface. **PTZ2** is among the very few small-molecule HTMs that can rival Spiro-OMeTAD in PSCs. The present work reveals the potential versatility of the phenothiazine building block for further development of inexpensive and efficient molecular HTMs for perovskite-based solar cells.

■ ASSOCIATED CONTENT

Supporting Information

The Supporting Information is available free of charge on the ACS Publications website at DOI: 10.1021/acsenergylett.7b00054.

Detailed synthetic procedures, characterization of all intermediates, and calculations for chemical cost; details of device construction and characterization (PDF)

■ AUTHOR INFORMATION

Corresponding Authors

*E-mail: roberto.grisorio@poliba.it.
*E-mail: antonio.abate@unifr.ch.

ORCID

Roberto Grisorio: 0000-0002-3698-9370
Bart Roose: 0000-0002-0972-1475
Antonio Abate: 0000-0002-3012-3541

Notes

The authors declare no competing financial interest.

■ ACKNOWLEDGMENTS

R.G. and G.P.S. acknowledge the Bridge-Early Stage COMPOSTRONICS project (cod. 5730587, Austrian Research Promotion Agency-FFG) and Italian MIUR for project MAAT (Molecular NAnotechnology for HeAlth and EnvironmenT; PON02_00563_3316357 − CUP B31C12001230005) for funding. S.C. and A.L. acknowledge Regione Puglia and ARTI for funding FIR: future in research projects "PeroFlex" (project no. LSBC6N4) and "HyLight" (project no. GOWMB21). A.A. and B.R. acknowledge the Adolphe Merkle and the Swiss National Science Foundation [Program NRP70 No. 153990].

■ REFERENCES

(1) Kojima, A.; Teshima, K.; Shirai, Y.; Miyasaka, T. Organometal Halide Perovskites as Visible-Light Sensitizers for Photovoltaic Cells. *J. Am. Chem. Soc.* **2009**, *131*, 6050−6051.

(2) Lee, M. M.; Teuscher, J.; Miyasaka, T.; Murakami, T. N.; Snaith, H. J. Efficient hybrid solar cells based on meso-superstructured organometal halide perovskites. *Science* **2012**, *338*, 643−647.

(3) Burschka, J.; Pellet, N.; Moon, S. J.; Humphry-Baker, R.; Gao, P.; Nazeeruddin, M. K.; Graetzel, M. Sequential deposition as a route to high-performance perovskite-sensitized solar cells. *Nature* **2013**, *499*, 316−319.

(4) Liu, M.; Johnston, M. B.; Snaith, H. J. Efficient planar heterojunction perovskite solar cells by vapour deposition. *Nature* **2013**, *501*, 395−398.

(5) Stranks, S. D.; Nayak, P. K.; Zhang, W.; Stergiopoulos, T.; Snaith, H. J. Formation of thin films of organic-inorganic perovskites for high-efficiency solar cells. *Angew. Chem., Int. Ed.* **2015**, *54*, 3240−3248.

(6) Jeon, N. J.; Noh, J. H.; Yang, W. S.; Kim, Y. C.; Ryu, S.; Seo, J.; Seok, S. I. Compositional engineering of perovskite materials for high-performance solar cells. *Nature* **2015**, *517*, 476−480.

(7) Saliba, M.; Orlandi, S.; Matsui, T.; Aghazada, S.; Cavazzini, M.; Correa-Baena, J. P.; Gao, P.; Scopelliti, R.; Mosconi, E.; Dahmen, K. H.; et al. A molecularly engineered hole-transporting material for efficient perovskite solar cells. *Nat. Energy* **2016**, *1*, 15017−15023.

(8) Krishnamoorthy, T.; Kunwu, F.; Boix, P. P.; Li, H.; Koh, T. M.; Leong, W. L.; Powar, S.; Grimsdale, A.; Graetzel, M.; Mathews, N.; Mhaisalkar, S. G. A swivel-cruciform thiophene based hole-transporting material for efficient perovskite solar cells. *J. Mater. Chem. A* **2014**, *2*, 6305−6309.

(9) Sung, S. D.; Kang, M. S.; Choi, I. T.; Kim, H. M.; Kim, H.; Hong, M.; Kim, H. K.; Lee, W. I. 14.8% perovskite solar cells employing carbazole derivatives as hole transporting materials. *Chem. Commun.* **2014**, *50*, 14161−14163.

(10) Choi, H.; Paek, S.; Lim, N.; Lee, Y. H.; Nazeeruddin, M. K.; Ko, J. Efficient Perovskite Solar Cells with 13.63% Efficiency Based on Planar Triphenylamine Hole Conductors. *Chem. - Eur. J.* **2014**, *20*, 10894−10899.

(11) Jeon, N. J.; Lee, J.; Noh, J. H.; Nazeeruddin, M. K.; Graetzel, M.; Seok, S. I. Efficient Inorganic−Organic Hybrid Perovskite Solar Cells Based on Pyrene Arylamine Derivatives as Hole-Transporting Materials. *J. Am. Chem. Soc.* **2013**, *135*, 19087−19090.

(12) Li, H.; Fu, K.; Hagfeldt, A.; Graetzel, M.; Mhaisalkar, S. G.; Grimsdale, A. C. A simple 3,4-ethylenedioxythiophene based hole-transporting material for perovskite solar cells. *Angew. Chem., Int. Ed.* **2014**, *53*, 4085−4088.

(13) Wang, J.; Wang, S.; Li, X.; Zhu, L.; Meng, Q.; Xiao, Y.; Li, D. Novel hole transporting materials with a linear π-conjugated structure for highly efficient perovskite solar cells. *Chem. Commun.* **2014**, *50*, 5829−5832.

(14) Krishna, A.; Sabba, D.; Li, H.; Yin, J.; Boix, P. P.; Soci, C.; Mhaisalkar, S. G.; Grimsdale, A. C. Novel hole transporting materials based on triptycene core for high efficiency mesoscopic perovskite solar cells. *Chem. Sci.* **2014**, *5*, 2702−2709.

(15) Abate, A.; Paek, S.; Giordano, F.; Correa-Baena, J.-P.; Saliba, M.; Gao, P.; Matsui, T.; Ko, J.; Zakeeruddin, S. M.; Dahmen, K. H.; et al. Silolothiophene-linked triphenylamines as stable hole transporting materials for high efficiency perovskite solar cells. *Energy Environ. Sci.* **2015**, *8*, 2946−2954.

(16) Cabau, L.; Garcia-Benito, I.; Molina-Ontoria, A.; Montcada, N. F.; Martin, N.; Vidal-Ferran, A.; Palomares, E. Diarylamino-substituted tetraarylethene (TAE) as an efficient and robust hole transport material for 11% methyl ammonium lead iodide perovskite solar cells. *Chem. Commun.* **2015**, *51*, 13980−13982.

(17) Do, K.; Choi, H.; Lim, K.; Jo, H.; Cho, J. W.; Nazeeruddin, M. K.; Ko, J. Star-shaped hole transporting materials with a triazine unit

DOI: 10.1021/acsenergylett.7b00054
ACS Energy Lett. 2017, 2, 1029−1034

for efficient perovskite solar cells. *Chem. Commun.* **2014**, *50*, 10971−10974.
(18) Cheng, M.; Chen, C.; Yang, X.; Huang, J.; Zhang, F.; Xu, B.; Sun, L. Novel Small Molecular Materials Based on Phenoxazine Core Unit for Efficient Bulk Heterojunction Organic Solar Cells and Perovskite Solar Cells. *Chem. Mater.* **2015**, *27*, 1808−1814.
(19) Kazim, S.; Ramos, F. J.; Gao, P.; Nazeeruddin, M. K.; Graetzel, M.; Ahmad, S. A dopant free linear acene derivative as a hole transport material for perovskite pigmented solar cells. *Energy Environ. Sci.* **2015**, *8*, 1816−1823.
(20) Liu, Y.; Chen, Q.; Duan, H. S.; Zhou, H.; Yang, Y.; Chen, H.; Luo, S.; Song, T. B.; Dou, L.; Hong, Z.; Yang, Y. A dopant-free organic hole transport material for efficient planar heterojunction perovskite solar cells. *J. Mater. Chem. A* **2015**, *3*, 11940−11947.
(21) Steck, C.; Franckevicius, M.; Zakeeruddin, S. M.; Mishra, A.; Bauerle, P.; Gratzel, M. A−D−A-type S,N-heteropentacene-based hole transport materials for dopant-free perovskite solar cells. *J. Mater. Chem. A* **2015**, *3*, 17738−17746.
(22) Xu, B.; Bi, D.; Hua, Y.; Liu, P.; Cheng, M.; Graetzel, M.; Kloo, L.; Hagfeldt, A.; Sun, L. A low-cost spiro[fluorene-9,9′-xanthene]-based hole transport material for highly efficient solid-state dye-sensitized solar cells and perovskite solar cells. *Energy Environ. Sci.* **2016**, *9*, 873−877.
(23) (b) Hua, Y.; Zhang, J.; Xu, B.; Liu, P.; Cheng, M.; Kloo, L.; Johansson, E. M. J.; Sveinbjörnsson, K.; Aitola, K.; Boschloo, G.; et al. Facile synthesis of fluorene-based hole transport materials for highly efficient perovskite solar cells and solid-state dye-sensitized solar cells. *Nano Energy* **2016**, *26*, 108−113.
(24) Malinauskas, T.; Saliba, M.; Matsui, T.; Daskeviciene, M.; Urnikaite, S.; Gratia, P.; Send, R.; Wonneberger, H.; Bruder, I.; Graetzel, M.; et al. Branched methoxydiphenylamine-substituted fluorene derivatives as hole transporting materials for high-performance perovskite solar cells. *Energy Environ. Sci.* **2016**, *9*, 1681−1686.
(25) Zhang, J.; Xu, B.; Johansson, M. B.; Vlachopoulos, N.; Boschloo, G.; Sun, L.; Johansson, E. M. J.; Hagfeldt, A. Strategy to Boost the Efficiency of Mixed-Ion Perovskite Solar Cells: Changing Geometry of the Hole Transporting Material. *ACS Nano* **2016**, *10*, 6816−6824.
(26) Gratia, P.; Magomedov, A.; Malinauskas, T.; Daskeviciene, M.; Abate, A.; Ahmad, S.; Graetzel, M.; Getautis, V.; Nazeeruddin, M. K. A Methoxydiphenylamine-Substituted Carbazole Twin Derivative: An Efficient Hole-Transporting Material for Perovskite Solar Cells. *Angew. Chem., Int. Ed.* **2015**, *54*, 11409−11413.
(27) Xu, B.; Sheibani, E.; Liu, P.; Zhang, J.; Tian, H.; Vlachopoulos, N.; Boschloo, G.; Kloo, L.; Hagfeldt, A.; Sun, L. Carbazole-Based Hole-Transport Materials for Efficient Solid-State Dye-Sensitized Solar Cells and Perovskite Solar Cells. *Adv. Mater.* **2014**, *26*, 6629−6634.
(28) Grisorio, R.; De Marco, L.; Baldisserri, C.; Martina, F.; Serantoni, M.; Gigli, G.; Suranna, G. P. Sustainability of Organic Dye-Sensitized Solar Cells: The Role of Chemical Synthesis. *ACS Sustainable Chem. Eng.* **2015**, *3*, 770−777.
(29) Zhang, F.; Liu, X.; Yi, C.; Bi, D.; Luo, J.; Wang, S.; Li, X.; Xiao, Y.; Zakeeruddin, S. M.; Graetzel, M. Dopant-Free Donor (D)−π−D−π−D Conjugated Hole-Transport Materials for Efficient and Stable Perovskite Solar Cells. *ChemSusChem* **2016**, *9*, 2578−2585.
(30) Malinauskas, T.; Tomkute-Luksiene, D.; Sens, R.; Daskeviciene, M.; Send, R.; Wonneberger, H.; Jankauskas, V.; Bruder, I.; Getautis, V. Enhancing Thermal Stability and Lifetime of Solid-State Dye-Sensitized Solar Cells via Molecular Engineering of the Hole-Transporting Material Spiro-OMeTAD. *ACS Appl. Mater. Interfaces* **2015**, *7*, 11107−11116.
(31) Liu, Y.; Hong, Z.; Chen, Q.; Chen, H.; Chang, W.-H.; Yang, Y.; Song, T.-B.; Yang, Y. Perovskite Solar Cells Employing Dopant-Free Organic Hole Transport Materials with Tunable Energy Levels. *Adv. Mater.* **2016**, *28*, 440−446.
(32) Trifiletti, V.; Roiati, V.; Colella, S.; Giannuzzi, R.; De Marco, L.; Rizzo, A.; Manca, M.; Listorti, A.; Gigli, G. NiO/$MAPbI_{3-x}Cl_x$/PCBM: A Model Case for an Improved Understanding of Inverted Mesoscopic Solar Cells. *ACS Appl. Mater. Interfaces* **2015**, *7*, 4283−4289.
(33) Saliba, M.; Matsui, T.; Seo, J.-Y.; Domanski, K.; Correa-Baena, J.-P.; Nazeeruddin, M. K.; Zakeeruddin, S. M.; Tress, W.; Abate, A.; Hagfeldt, A.; et al. Cesium-containing triple cation perovskite solar cells: improved stability, reproducibility and high efficiency. *Energy Environ. Sci.* **2016**, *9*, 1989−1997.
(34) Christians, J. A.; Manser, J. S.; Kamat, P. V. Best Practices in Perovskite Solar Cell Efficiency Measurements. Avoiding the Error of Making Bad Cells Look Good. *J. Phys. Chem. Lett.* **2015**, *6*, 852−857.

DOI: 10.1021/acsenergylett.7b00054
ACS Energy Lett. 2017, 2, 1029−1034